11th International Symposium on Magnetic Bearings
August 26-29, Nara, Japan

DYNAMIC PERFORMANCE LIMITATION IN DRIVING A RADIAL AMB WITH SPACE VECTOR PWM

Hyeong-Joon Ahn
Dept. of Mechanical Eng., Soongsil University, Seoul, 156-743 Korea
email: ahj123@ssu.ac.kr

ABSTRACT

As the uses of inverters with small AC motors are increasing rapidly, the power stage of these inverters has been designed to meet the efficiency, reliability, size, and cost constraints of the end products. The proven technologies of the AC drive industry have, however, rarely been applied to active magnetic bearing (AMB) systems. This paper presents dynamic performance limitation in driving a radial AMB using space-vector pulse width modulation (SVPWM), which is one of the most popular and favorable PWM schemes in the AC drive industry. The voltage and current of two coils for a single axis AMB are controlled independently through the SVPWM technique just like a two-phase motor. Two driving configurations, full performance and economy configurations, are proposed. In particular, the economy configuration is found to be more cost-effective than the half-bridge scheme. Conversion rules for two coil voltages of an AMB into the three-leg converter voltages are developed for both driving configurations. Finally, the dynamic performance limitations of the proposed driving configurations are investigated both analytically and numerically, which shows that proper coil connection architecture for a radial AMB can minimize the dynamic performance degradation of the proposed driving methods

INTRODUCTION

The cost and reliability of sophisticated control electronics remain the main obstacles to the widespread of AMB systems, although these systems have many advantages, e.g. non-contact, lubricant-free operation, high rotational speeds and flexibility in choosing bearing characteristics [1-3]. In particular, the cost of power amplifiers is a large portion of the whole system. For example, turbo-molecular pumps whose production rates are in the order of 25 units per day need 10 independent power amplifiers per pump.

Proven technologies of the AC drive industry, such as integrated power devices and control architectures, have rarely been applied to AMB systems. The power stage of these inverters must meet the efficiency, reliability, size, and cost constraints of the end products, since the use of inverters with small AC motors in appliances and low power industrial applications is increasing rapidly. So far, various insulated gate bipolar transistor (IGBT) power modules have been designed to provide a cost-effective solution by combining optimized drive integrated circuits and power devices into a single package [4, 5]. Moreover, traditional sinusoidal pulse width modulation (PWM) technique is being replaced by a space-vector PWM (SVPWM) technique. The SVPWM has proven to be one of the most popular and favorable PWM schemes and extensive research on SVPWM has been done in the past few decades [6-8].

Although AMB research and development have advanced over a span of 60 years, only a little research has been done on power amplifiers for AMB systems. Most current AMB systems adopt efficient switching power amplifiers because linear power amplifiers have low efficiency [9]. A synchronous three-level PWM power amplifier was proposed, having low current harmonics even with low switching frequency [10]. A three-phase converter was applied to both a three-pole and a twelve-pole radial AMB systems, which in both cases needed complex winding and suffered from cross-coupling [11, 12]. In addition, several digital control schemes for low-cost industrial AMB applications were discussed including a simple voltage control [13]. It is still, however, very important to develop a cost-effective and reliable power amplifier appropriate to an advanced digital controller.

This paper presents dynamic performance limitation in driving a radial AMB using SVPWM. The voltage and current of two coils for single axis AMB are controlled independently using the SVPWM technique just as for a two-phase motor. Two driving configurations: full

performance and economy configurations are proposed. As will be shown, the economy configuration is more cost-effective than the half bridge scheme. Conversion rules of AMB coil voltages into the three-leg converter voltages are developed for both driving configurations. Finally, the dynamic performance limitations of the proposed driving configurations are analyzed in both mathematical and numerical ways. The analysis results show that proper coil connection architecture for a radial AMB can prevent large dynamic performance degradations of the proposed driving configurations.

AMB AND ITS POWER AMPLIFIER

An AMB system usually consists of electromagnets, a target, position sensors, power amplifiers and a position controller. Although the AMB system is unstable in open-loop status, the target can be stably supported by controlling the currents of the electromagnets, using the measured displacement of the target. The AMB power amplifier converts a weak control signal into a physical quantity such as current or voltage that produces a magnetic force. The most common power amplifier is a current control with differential driving mode, as shown in Figure 1. In this case, the position controller produces the control current (i_c) using the measured target displacement (y) and the current controllers produce appropriates voltages (V_1 and V_2) of the coils. The AMB system adds a bias current (i_b) to the control current in order to linearize the current-force relationship and to increase the dynamic stiffness [1]. Moreover, the single degree of freedom (DOF) AMB with respect to the linearized magnetic force can is physically well-represented by the one dimensional vibration of a mass-spring-damper system.

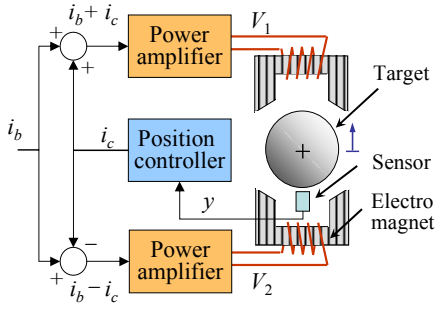

FIGURE 1: A single degree of freedom AMB system

Figure 2 shows three typical driving configurations for AMB systems. The most cost-effective scheme is the half-bridge scheme in Figure 2(a). Two DC sources of half amplitude are built up by splitting the DC link voltage with two capacitors. Thus, the balance of the two split DC voltages must carefully be maintained by increasing the capacitor volume or by an active control. The full-bridge scheme can use the whole DC link voltage. This scheme, however, requires twice as many switch elements as the half-bridge scheme, as shown in Figure 2(b). A cost-effective modified full-bridge scheme was introduced taking into account the one-directional current flow of AMB, as shown in Figure 2(c).

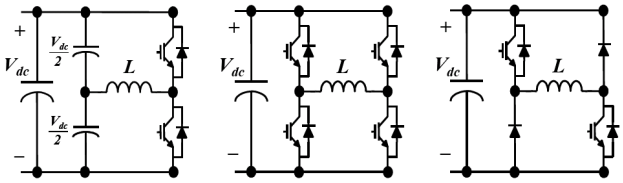

FIGURE 2: Driving configurations for AMB systems (a) Half-bridge (b) Full-bridge (c) Modified full-bridge

The full-bridge configuration has much better performance than the half-bridge configuration. The output voltage of the half-bridge configuration can be significantly distorted if the desired voltage output is greater than half of the DC link voltage. In addition, the maximum current slew rate of the half-bridge is just half that of the full-bridge configuration.

DRIVING AN AMB USING SVPWM

Driving configurations

A two-phase AC motor is composed of two symmetrical windings, which are electrically 90 degrees out of phase with one another. The two-phase motor can be driven using a three-leg voltage source converter shown in Figure 3. The three-leg voltages of V_a, V_b and V_c according to the switching states of S_a, S_b and S_c determine the two coil voltages of the motor independently, which is called as a two-dimensional space vector modulation [14].

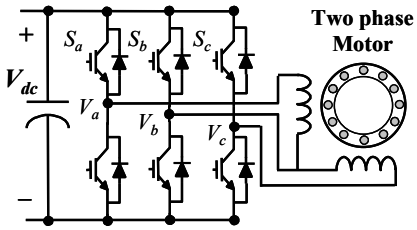

FIGURE 3: Driving a two-phase motor with a three-leg

voltage converter

Since the single DOF AMB system shown in Figure 1 has two coils like a two-phase motor, a three-phase inverter can drive a single DOF AMB system with two different driving configurations: full performance and economy configurations, as shown in Figure 4. In particular, the three of the switching devices can be saved in the economy configuration since the coil current of an AMB system flows in one direction, which essentially is the same principle of operation as the modified full-bridge shown in Figure 2(c). The economy configuration is, therefore, more cost-effective than both the half-bridge and the modified full-bridge schemes, since the proposed scheme requires only one and half switches per coil.

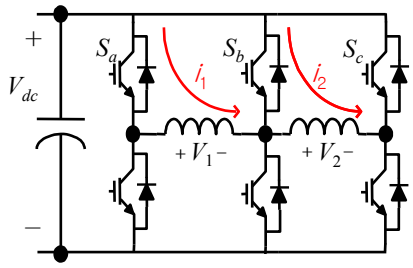

(a) Full peformance driving configuration

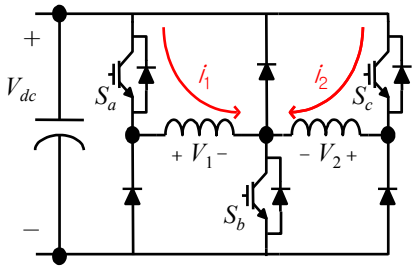

(b) Economy driving configuration

FIGURE 4: Driving configurations of a three phase inverter for an AMB system

In the proposed driving configurations, there are eight switching states: six active states and two zero states. The coil voltages vary according to the switching states. The relationships between the switching states and the two coil voltages are shown in Table 1. There are unavailable voltage pairs for two configurations: ($+V_{dc}$, $+V_{dc}$) and ($-V_{dc}$, $-V_{dc}$) for the full performance configuration, and ($+V_{dc}$, $-V_{dc}$) and ($-V_{dc}$, $+V_{dc}$) for the economy configuration.

TABLE 1: Relationship between the switching states and the coil voltages

Switching states			Full performance		Economy	
S_a	S_b	S_c	V_1	V_2	V_1	V_2
0	0	0	0	0	$-V_{dc}$	$-V_{dc}$
0	0	1	0	$-V_{dc}$	$-V_{dc}$	0
0	1	0	$-V_{dc}$	$+V_{dc}$	0	0
0	1	1	$-V_{dc}$	0	0	$+V_{dc}$
1	0	0	$+V_{dc}$	0	0	$-V_{dc}$
1	0	1	$+V_{dc}$	$-V_{dc}$	0	0
1	1	0	0	$+V_{dc}$	$+V_{dc}$	0
1	1	1	0	0	$+V_{dc}$	$+V_{dc}$

A voltage reference vector for the two coil voltages can be obtained using the SVPWM technique by the interpolation of two adjacent active state and a zero state vectors. Available voltage regions for the two coils of an AMB using the SVPWM technique are shown in Figure 5. Six voltage regions are grouped into three sectors and the conversion rules of the coil voltages into the three-leg voltages are developed in Tables 2 and 3, respectively. Here, a and b are the normalized coil voltages V_1/V_{dc} and V_2/V_{dc}, respectively and V_a, V_b and V_c are the three-leg voltage of the converter shown in Figure 3.

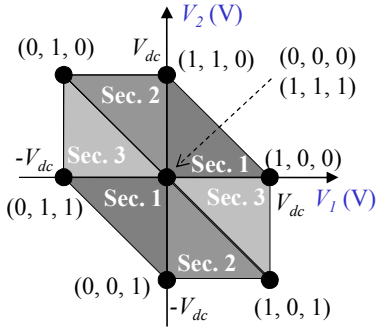

(a) The full peformance configuration

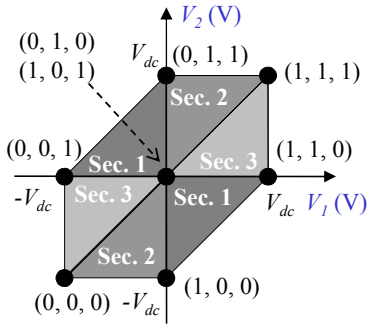

(a) The economy peformance configuration

FIGURE 5: Available voltage region of two driving configurations

TABLE 2: Conversion rules of the coil voltages into the three-leg voltages for the full performance driving configuration

Sec.	$a(a\text{-}b)>0$	$ab>0$	V_a/V_{dc}	V_b/V_{dc}	V_c/V_{dc}
1	*	T	$(1+a+b)/2$	$(1-a+b)/2$	$(1-a-b)/2$
2	T	F	$(1+2a+b)/2$	$(1+b)/2$	$(1-b)/2$
3	F	F	$(1+a)/2$	$(1-a)/2$	$(1-a-2b)/2$

TABLE 3: Conversion rules of the coil voltages into the three-leg voltages for the economy driving configuration

Sec.	$a(a\text{-}b)>0$	$ab>0$	V_a/V_{dc}	V_b/V_{dc}	V_c/V_{dc}
1	*	F	$(1+a-b)/2$	$(1-a-b)/2$	$(1-a+b)/2$
2	F	T	$(1+2a-b)/2$	$(1-b)/2$	$(1+b)/2$
3	T	T	$(1+a)/2$	$(1-a)/2$	$(1-a+2b)/2$

Driving a radial AMB

A heteropolar radial AMB is most widely used in rotating machinery applications and has four electromagnets (EM), as shown in Figure 6 [15]. Therefore, two three-leg voltage converters are required in order to drive a radial AMB. Usually, two opposing electromagnets differentially generate one directional force (F_1 or F_2), and control currents of the opposing electromagnets have a 180 degree phase difference. In addition, the phase difference of two perpendicular forces (F_1 and F_2) is 90 degrees in order to compensate for the unbalanced harmonic forces of the rotor.

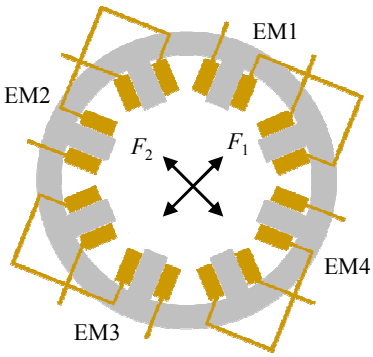

FIGURE 6: A heteropolar radial AMB

There are two possible coil connection architectures for a radial AMB driven by a three-leg voltage converter; two opposing electromagnets (EM1 and EM3; EM2 and EM4) or two adjacent electromagnets (EM1 and EM2; EM3 and EM4) are driven by a three–leg voltage converter. If the two opposing electromagnets are driven by a three–leg voltage converter, the current phases of the two coils are normally 180 degrees apart in order to generate a force. Then, the three-leg voltage converter is expected to spend the most time in second and forth quadrants, shown as a solid straight line in Figure 7. On the other hand, the coil current phases of adjacent electromagnets are necessarily 90 degrees apart in order to produce a harmonic force and the corresponding coil voltages are 90 degrees phase apart, which describes the dashed circle in Figure 7. In addition, the available voltage region of the full-bridge scheme with the same DC link voltage is shown as a gray rectangle in Figure 7.

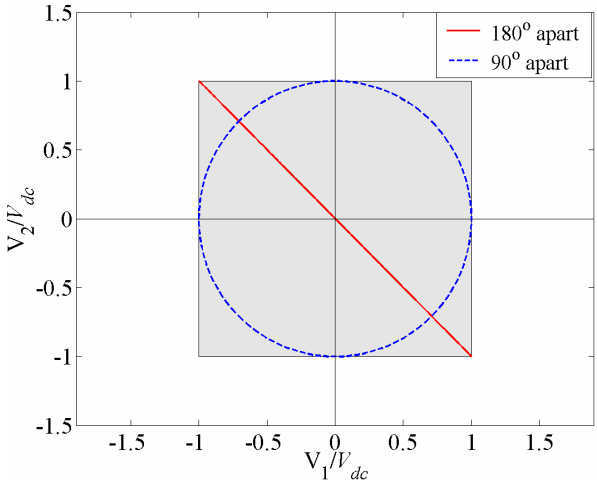

FIGURE 7: Voltage space of driving a radial AMB

Both the full performance and the economy driving configuration have smaller voltage regions than the full-bridge configuration, which may lead to the dynamic performance limitation in driving a radial AMB; the proper coil connection architecture for a radial AMB can, however, minimize the dynamic performance degradations of two driving configurations. If two opposing electromagnets (180 degrees apart) are driven by the full performance driving configuration, there is no performance degradation. However, if adjacent electromagnets (90 degrees apart) are driven by the full performance driving configuration, a small degradation in dynamic performance appears due to the reduced voltage region. On the other hand, if two opposing electromagnets are driven by the economy driving configuration, the dynamic performance is significantly restricted. However, when adjacent electromagnets (90 degrees apart) are driven by the economy driving configuration, the performance degradation is the same as that experienced by the full performance driving used for adjacent electromagnets.

ANALYSIS OF DYNAMIC PERFORMANCE LIMITATION

Sinusoidal voltage generation

Simulations of sinusoidal voltage generation are performed in order to investigate the sinusoidal voltage and current profiles of the two driving configurations. Simulink models of two driving configurations are built as shown in Figure 8: the driven coil has a resistance of 1.5Ω and inductance of 8mH. The DC link voltage and switching frequency are 50V and 1 kHz, respectively. The PWM voltages are filtered to produce a smooth voltage signal.

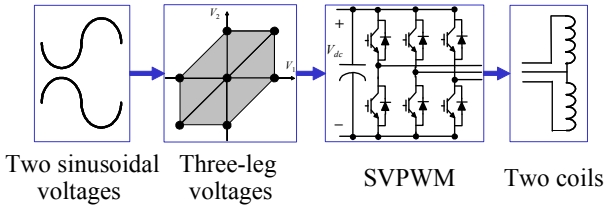

FIGURE 8: Block diagram of the simulation model

In both coil connection architectures, sinusoidal voltages of 50V amplitude and 10 Hz frequency are generated by each driving configuration. The filtered output PWM voltages are shown in Figure 9. If the full-bridge or the full performance driving configuration drives the opposing electromagnets, a complete sinusoidal voltage can be produced without any distortion, which is shown as a dotted curve in Figure 9. That is because the voltage region of the full performance configuration in Figure 5(a) completely covers the second and forth quadrants despite reduced voltage region in both first and third quadrants. If adjacent electromagnets (90 degrees phase apart) are driven by the full-performance or the economy driving configuration, slightly-distorted sinusoidal voltage as depicted by the solid lines in Figure 9 are generated. In particular, the sinusoidal voltages are distorted when the voltage regions in Figure 5 cannot cover the voltage region encompassed by the dashed circle in the Figure 7. In contrast, the economy driving configuration, when applied to the opposing electromagnets, produces a significantly-distorted sinusoidal voltage, which is shown as the dashed curve in Figure 9.

Corresponding current profiles of the two driving configurations are shown in Figure 10. The corresponding current signals are also distorted by the voltage signal distortion shown in Figure 9. In particular, the current of either the full performance or economy driving configuration for the adjacent electromagnets has slightly smaller peaks than that of the full-bridge configuration. This leads to a small degradation in the dynamic performance [16].

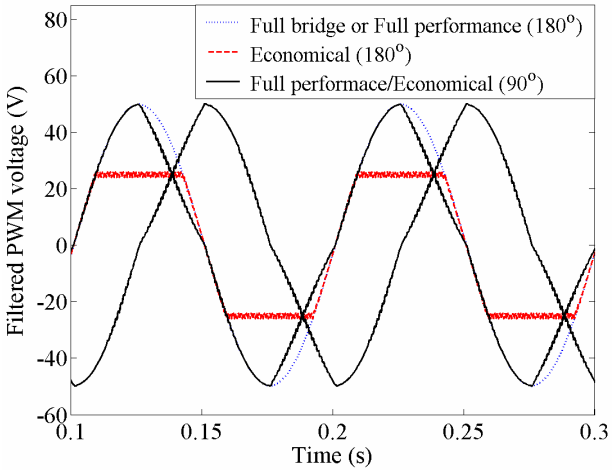

FIGURE 9: Voltage profiles of the driving configurations for a radial AMB

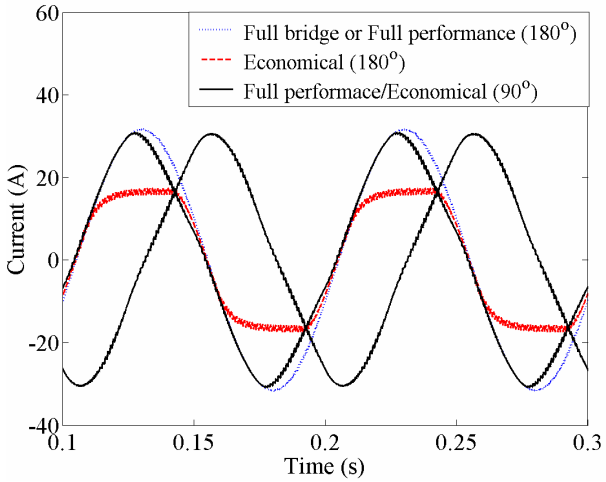

FIGURE 10: Current profiles of the driving configurations for a radial AMB

Mathematical analysis

The dynamic performance degradations of the driving configurations are mathematically analyzed in this section. The worst case among the driving configurations is the economy configuration that is used to drive the opposing electromagnets. It is clearly seen to have just half the dynamic performance due to its having half the DC link voltage. However, evaluation of the dynamic performance degradation is not obvious when the

adjacent electromagnets are driven by either the full performance or the economy driving configuration, which is analyzed mathematically.

A coil of an AMB system can be modeled as a connection of resistance, R, and inductance, L, in series. Current, i, with a sine wave voltage input of amplitude, V, and frequency, ω, can be obtained through solving the differential equation below.

$$L\frac{di}{dt}+Ri=V\sin\omega t \tag{1}$$

A steady-state solution of the differential equation is

$$i(t)=\frac{V}{L^2\omega^2+R^2}\left(R\sin\omega t-L\omega\cos\omega t\right) \tag{2}$$

We assume the worst voltage profile like the solid line in Figure 9. Since the voltage profile is sine wave before $t=\pi/2\omega$, the current at $t=\pi/2\omega$ should be $VR^2/(L^2\omega^2+R^2)$ from Eq. (2). The differential equation after $t=\pi/2\omega$ can be expressed by Eq. (3) considering the clamped voltage profile.

$$L\frac{di}{dt}+Ri=\frac{2V\omega}{\pi}\left(\frac{\pi}{\omega}-t\right),\ i\left(\frac{\pi}{2\omega}\right)=\frac{VR}{L^2\omega^2+R^2} \tag{3}$$

The solution of the differential equation after applying the initial condition is given by

$$i(t)=-\frac{V}{R}\left(\frac{L^2\omega^2}{L^2\omega^2+R^2}+\frac{2\omega}{\pi}\frac{L}{R}\right)e^{\frac{R}{L}\left(\frac{\pi}{2\omega}-t\right)}+\frac{V}{R}\frac{2\omega}{\pi}\left(\frac{\pi}{\omega}+\frac{L}{R}-t\right) \tag{4}$$

The current has the maximum value when the differentiation of the solution is zero. The time when the differentiation of Eq. (4) is zero can be expressed by

$$t=\frac{L}{R}\ln\left(1+\frac{\pi}{2\omega}\frac{R}{L}\frac{L^2\omega^2}{L^2\omega^2+R^2}\right)+\frac{\pi}{2\omega} \tag{5}$$

The maximum current can be calculated by substituting the time into Eq. (4).

$$i_{\max}=\frac{V}{R}\left(1-\frac{2\omega}{\pi}\frac{L}{R}\ln\left(1+\frac{\pi}{2\omega}\frac{R}{L}\frac{L^2\omega^2}{L^2\omega^2+R^2}\right)\right) \tag{6}$$

The peak current is normalized dividing the currents by a factor of V/R and replacing $\omega L/R$ as τ. The peak currents of the two driving configurations can then be rewritten as in Eq. (7). The normalized peak current and the relative dynamic performance degradation for various τ values are calculated and shown in Figure 11. The relative performance degradation increases as the value of τ increases. In addition, the value of τ is generally less than 10, and the maximum performance degradation of the proposed scheme is less than 20%.

$$\begin{matrix}\dfrac{1}{\sqrt{\tau^2+1}} & \text{the full performance}\\ 1-\dfrac{2}{\pi}\tau\ln\left(1+\dfrac{\pi}{2}\dfrac{\tau}{\tau^2+1}\right) & \text{the performance degradation}\end{matrix} \tag{7}$$

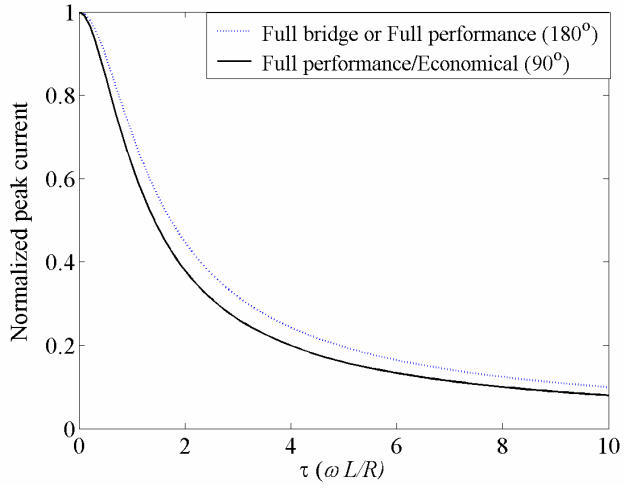

(a) Normalized peak currents of driving configurations

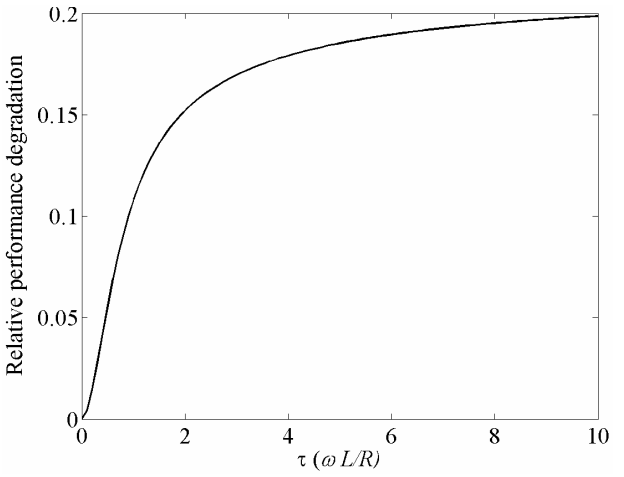

(b) Relative performance degradation of the economy driving configuration

FIGURE 11: Performance degradation of driving configurations

Simulations

Simulations of sinusoidal voltage generation are performed in order to verify the dynamic performances of the proposed driving configurations. First, the output voltage total harmonic distortions (THD) of two driving configurations are investigated numerically. The coil parameters are the same in section 4.1. The modulation index or normalized amplitude is varied from 0.1 to 1, and the non-dimensional frequency (since wave frequency/switching frequency) is varied from 0.01 to 0.1.

The output voltage THDs of the two driving configurations according to the modulation index are shown in Figure 12. If the opposing electromagnets of a radial AMB are driven by the economy driving configuration, the output voltage is significantly distorted, as the modulation index becomes larger than 0.5, i.e. half the DC link voltage. In addition, the THD of the output voltage for adjacent electromagnets of a radial AMB using either the driving configuration becomes larger than the full-bridge configuration as the modulation index increases beyond 0.71 ($1/\sqrt{2}$). The performance degradation rate, however, is much smaller than that of the economy driving configuration for the opposing electromagnets.

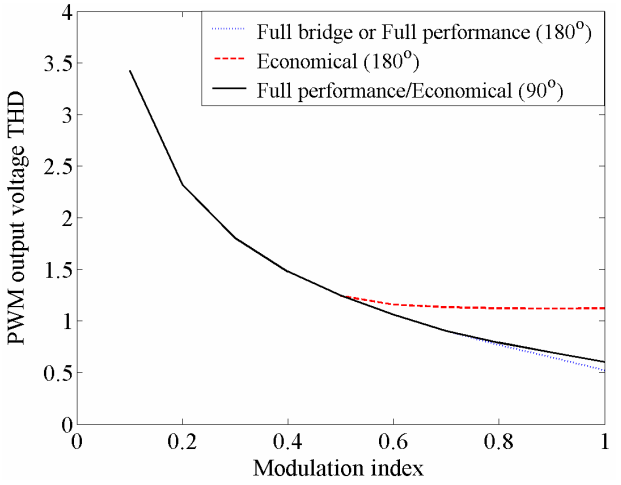

FIGURE 12: Output voltage THDs for various modulation indexes

The peak currents of both the driving configurations for the coil connection architectures of a radial AMB are calculated according to the modulation index and shown in Figure 13. The peak currents of the economy driving configuration appear to be smaller than those of the full-bridge driving configuration when the modulation index values are greater than 0.71, which is because of the reduced voltage space shown in Figure 7.

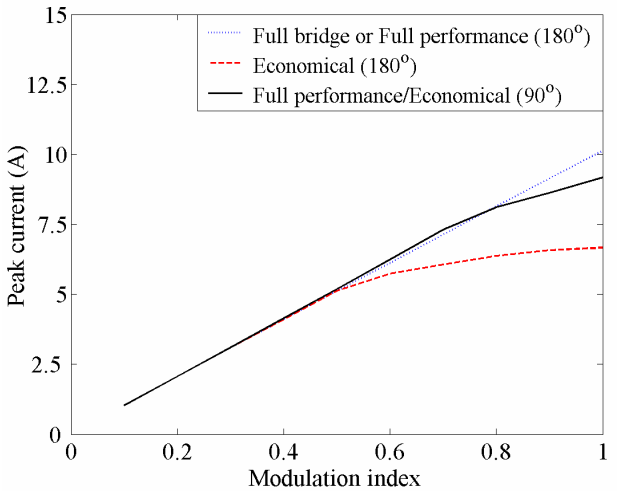

FIGURE 13: Peak currents for various modulation indexes

The peak currents of both the driving configurations for the coil connection architectures of a radial AMB are calculated according to the normalized frequency and shown in Figure 14. The results of the mathematical analysis and simulation results agree well with one another.

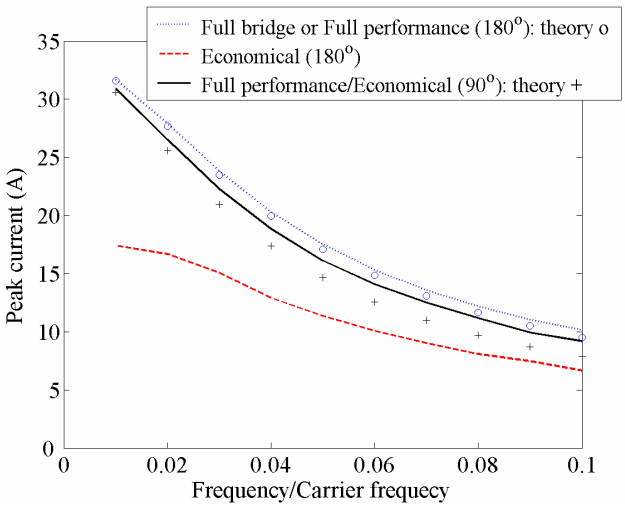

FIGURE 14: Peak currents for various frequencies

CONCLUSION

This paper presents dynamic performance limitation in driving a radial AMB using SVPWM. The voltage and current of two coils for a single axis AMB are controlled

independently through the SVPWM technique, just as would be done for a two-phase motor. Two driving configurations are proposed: full performance and economy configurations. The economy configuration is more cost-effective than the half-bridge scheme. Conversion rules for two coil voltages of an AMB into the three-leg converter voltages are developed for both driving configurations. The dynamic performance limitations of the proposed driving configurations are discussed both analytically and numerically. The results show that suitable coil connection architecture for a radial AMB can minimize the dynamic performance degradation of either driving configuration.

REFERENCES

1. Schweitzer, G., Bleuler, H. and Traxler, A.,"Active Magnetic Bearings," Hochschulverlag AG an der ETH Zurich, 1994.

2. Ahn, H.J. and Han, D.C., "System Modeling and Robust control of an AMB spindle : Part II Mu controller design and implementation," KSME international, 17(12), pp. 1844-1854, 2003.

3. Ahn, H.J. and Han, D.C., "System Modeling and Robust control of an AMB spindle : Part I Modeling and validation for robust control," KSME international, 17(12), pp. 1855-1866, 2003.

4. Powerex. Inc., "IPM Family Application Note," 200 Hillis Street, Youngwood, Pennsylvania 15697-1800, 2001.

5. Fairchild semiconductor inc., "Smart Power Module User's guide," Application note 9018, September, 2001.

6. Joachim, H., "Pulsewidth Modulation - A Survey," IEEE Transactions on Industrial electronics, Vol. 39, No. 5, pp. 410-420, 1992.

7. van der Broeck, H. W., Skudelny, H. C., and Stanke, G., "Analysis and realization of a pulsewidth modulator base on voltage space vectors," IEEE Transactions on Industrial Applications, Vol. 24, pp. 142-150, 1988.

8. Chung, D-W, Kim, J-S, and Sul, S-K, "Unified Voltage Modulation Technique for Real-Time Three-Phase Power Conversion," IEEE Trans. on Industry Applications, Vol. 34, No. 2, Mar./Apr., pp. 374-380, 1998.

9. Keith, F. J., Maslen, E. H. ,Humphris, R. R., and Williams, R. D., "Switching Amplifier Design for Active Magnetic Bearings," Proc. 2nd International Symposium on Magnetic bearings, Tokyo, Japan, pp. 211-218, July 12-14, 1990.

10. Zhang, J., "Power Amplifier for Active Magnetic Bearings," Ph.D. dissertation, ETH Zurich, Switzerland, 1995.

11. Schob, R., Redemann, C. and Gempp, T., "Radial Active Magnetic Bearing for Operation with a 3-Phase Power Converter," Proc. 4th International Symposium on Magnetic Suspension Technology; Gifu, Japan, pp. 111-124, 1997.

12. Gempp, T., Redemann, C. and Schob, R., "Active Magnetic Bearing with Large Air Gap for Operation with a 3-phase Power Converter," Proc. of Int. Gas Turbine & Aeroengine Congress & Exhibition, Indianapolis, 99-GT-204, 1999.

13. Buhler, P., Siegwart, R. and Herzog, R., "Digital Control for Low Cost Industrial AMB Applications," 5th international symposium on Magnetic bearings, Aug., Kanazawa, Japan, pp. 83-88, 1996.

14. Jang, D.-H., and Yoon, D.-Y., "Space-vector PWM technique for two phase inverter-Fed two-phase induction motors," IEEE transactions on industrial applications, Vol. 39 (2), pp. 542-549, 2003.

15. Noh, M., "A Model of Magnetic Bearings Considering Eddy Currents and Hysteresis," International Journal of Precision Engineering and Manufacturing, Vol.4 No.3, pp.5-11, 2003.

16. Maslen, E. H., Hermann, P., Scott, M. A., and Humphris, R. R., "Practical Limits to the Performance of Magnetic Bearings: Peak Force, Slew Rate, and Displacement Sensitivity," ASME Journal of Tribology, vol. 111, no. 2, pp. 33